BIOCHEMISTRY
including biophysical chemistry & molecular biology
Article

Biochemistry **2009,** *48,* 10129–10135 10129
DOI: 10.1021/bi900928n

Observation of the Membrane Binding Activity and Domain Structure of gpV, Which Comprises the Tail Spike of Bacteriophage P2[†]

Yasuhiro Kageyama,[‡] Masanori Murayama,[‡] Takashi Onodera,[‡] Seiko Yamada,[‡] Harumi Fukada,[§] Motonori Kudou,[∥] Kouhei Tsumoto,[∥] Yoshiharu Toyama,[‡] Syunsaku Kado,[‡] Kenji Kubota,[‡] and Shigeki Takeda*[,‡]

[‡]*Department of Chemical Biology, Graduate School of Engineering, Gunma University, 1-5-1 Tenjin-cho, Kiryu, Gunma 376-8515, Japan,* [§]*Graduate School of Agriculture and Biological Sciences, Osaka Prefecture University, Sakai, Osaka 599-8531, Japan, and* [∥]*Department of Medical Genome Sciences, Graduate School of Frontier Sciences, The University of Tokyo, 301 FBS-Building, 5-1-5 Kashiwanoha, Kashiwa 277-8562, Japan*

Received June 2, 2009; Revised Manuscript Received September 23, 2009

ABSTRACT: The P2 phage virion has tail spike proteins beneath the baseplate and uses them to adsorb to the outer membrane of *Escherichia coli* during the infection process. Previous immunoelectron microscopic studies suggested that the tail spikes are composed of the gene V product (gpV); however, experimental evidence of its membrane binding activity has yet to be reported. In this study, we purified and characterized recombinant full-length gpV and its C-terminal domain. Limited chymotrypsin proteolysis of gpV produced a C-terminal domain composed of Ser86−Leu211. Our experiments demonstrated that the N- and C-terminal domains have very different melting temperatures: 50 and 74 °C, respectively. We also found that gpV binds the *E. coli* membrane via its C-terminal domain. We conclude that the C-terminal domain of gpV is a stable trimer and serves as the receptor-binding domain for the second step in the phage adsorption process.

Bacteriophage P2, one of the most typical *Myoviridae*, is a temperate phage consisting of a head, a contractile tail, and tail fibers. Recent genome projects have revealed that P2-like prophages are frequently encountered and are common in the genomes of proteobacteria (*1*). Therefore, P2-like phages are thought to play an important role in horizontal gene transfer (*2*). This is also indicated by the fact that P2-like phage binds several different cell membrane surfaces during its infection processes. The *Myoviridae* adsorption process consists of two temporal steps (*3*). The first step is the specific recognition between the phage (long) tail fibers and the receptor, which is distributed over the host cell surface. Although this first binding step is reversible for many phages, the host selectivity of the phages is determined by their tail fiber specificity. In several myoviruses, mutation or replacement of tail fiber proteins induces switching of the host range (*4*). For the second binding step, many phages use dedicated spike proteins located beneath the tail baseplate to reach their host cells. Because these tail spike proteins form strong and irreversible bonds, tail spike specificity is as important for the infection process and host recognition as the specificity of tail fibers. To understand host adhesion and infection systems, purification and characterization of the receptor-binding proteins of the phages are necessary. Receptor-binding domains of the tail spike proteins of P22 (*5*) and Det7 phages (*6*) and the short tail fibers of T4 phages (*7*) have been reported. All form trimers based on a β-helical structure and bind to host lipopolysaccharides. The receptor-binding domains are located at the C-termini of the primary structures. Since the gene V product (gpV)[1] of P2 phage is a component of the baseplate and was found to be located on the lateral face of the baseplate by electron microscopy (*8*), it is thought to function as a tail spike. On the other hand, P2 gpV does not share any sequence homology with the tail spikes of the phages mentioned above, whose structures have been determined. Moreover, direct experimental evidence of the membrane binding activity of gpV has yet to be reported. Finally, it was reported that P2 gpV is composed of 211 amino acids per subunit, and a Gly64Glu mutation in P2*ts*199 resulted in a temperature-sensitive (*ts*) phenotype, with growth at 30 °C but not at 42 °C. The C-terminal region (residues 142−207) of P2 gpV shares significant homology (45.5%) with Mu phage gp45, which is also predicted to be a tail spike protein, although its structure has not yet been determined.

In this paper, we present the first measurement of the membrane binding properties of gpV. We purified the C-terminal proteolytic fragment of gpV and found that its C-terminal domain binds host cell membranes and that it exists as a stable trimer. These results indicate that the behavior of gpV is similar to that of the tail spike proteins of other phages. Therefore, we conclude that gpV is a receptor-binding protein involved in the second step of phage adsorption.

[†]This work was supported by a Grant-in-Aid for Scientific Research from the Ministry of Education, Science, Sports, and Culture of Japan (to S.T.).

*To whom correspondence should be addressed: Department of Chemical Biology, Graduate School of Engineering, Gunma University, 1-5-1 Tenjin-cho, Kiryu, Gunma 376-8515, Japan. Telephone or fax: +81-277-30-1434. E-mail: stakeda@chem-bio.gunma-u.ac.jp.

[1]Abbreviations: DSC, differential scanning calorimetry; gpV, gene product of gene V; gpV-C, C-terminal fragment of gpV (Ser87−Leu211); IPTG, isopropyl 1-thio-β-D-galactosidase; PMSF, phenylmethanesulfonyl fluoride; PBS, phosphate-buffered saline; PCR, polymerase chain reaction; QCM, quartz crystal microbalance; SAM, self-assembling monolayer; SDS−PAGE, sodium dodecyl sulfate−polyacrylamide gel electrophoresis; T_m, melting temperature; Tris, tris(hydroxymethyl)aminomethane; *ts*, temperature-sensitive mutant that grows at 30 °C but not at 42 °C.

Published on Web 09/25/2009

MATERIALS AND METHODS

Strains and Media. gpV expression plasmid pEE670, kindly donated by E. Haggård-Ljungquist (University of Stockholm, Stockholm, Sweden), is derived from pET16b and carries gene V fused in-frame to a histidine tag (*8*). We constructed mutants and truncated gene V by polymerase chain reaction using KOD plus polymerase (Toyobo) and inserted them into pEE670 in place of wild-type gene V. *Escherichia coli* XL1-Blue and BL21(DE3)-pLysS were used for the construction of mutant genes and overexpression, respectively. Luria broth (10 g of Bacto tryptone, 5 g of yeast extract, and 10 g of NaCl per liter of water) was used to cultivate XL1-Blue and BL21(DE3)pLysS.

Overexpression and Purification. Transformed *E. coli* cells were grown at 37 °C in Luria broth containing 100 μg/mL ampicillin for expression of the wild-type, Gly64Ala, and Gly-64Leu versions of gpV, as well as the C-terminal domain fragment (Ser87−Leu211) (gpV-C). For expression of Gly64Lys, cultivation was performed at 20 °C. Expression of gene V was induced with 1 mM isopropyl β-D-thiogalactopyranoside (IPTG) when the turbidity of the medium at 600 nm reached 0.8. The cells were harvested by centrifugation at 7000 rpm for 10 min after cultivation for at least an additional 3 h, followed by suspension in 10 mM Tris-HCl (pH 8.0) and 1 mM EDTA. After sonication (three 5 min cycles at 60 W) in the presence of 1 mM phenylmethanesulfonyl fluoride (PMSF) and centrifugation (6000 rpm for 10 min), the supernatant was recovered and dialyzed twice against 50 mM Tris-HCl (pH 8.0). The dialyzed sample was loaded onto a DEAE-Toyopal (Tosho) anion-exchange column (100 mL) equilibrated with 50 mM Tris-HCl (pH 8.0). Proteins were eluted with a linear gradient of NaCl from 0 to 0.5 M, followed by washing with 50 mM Tris-HCl (pH 8.0). The fractions containing gpV were dialyzed twice against 20 mM phosphate (pH 7.4) and 500 mM NaCl and then loaded onto a nickel-affinity column (5 mL, Pharmacia) equilibrated with dialysis buffer. After sample loading, the column was washed with 20 mL of 20 mM phosphate (pH 7.4) and 50 mM imidazole, and gpV was eluted with 20 mM phosphate (pH 7.4) and 500 mM imidazole. The gpV fractions were concentrated with Amicon ultrafiltration cells with YM-30 filters (Millipore) followed by purification on a Sephacryl S-300 (Bio-Rad) gel-filtration column (400 mL) equilibrated with 50 mM Tris-HCl (pH 7.4) and 500 mM arginine. All of the purification procedures described above were conducted at 4 °C. The protein concentration was monitored by the absorbance at 280 nm, and the proteins were subjected to 15% SDS−PAGE. The gpV and gpV-C concentrations were calculated using extinction coefficients at 280 nm of 1.11 and 0.084, respectively, which were estimated from their amino acid compositions.

Limited Proteolysis. Limited proteolysis was performed using chymotrypsin (Sigma) with a weight ratio of 1:50 in a plastic tube with 150 μL of gpV (0.19 mg/mL) dissolved in 10 mM Tris-HCl (pH 8.0), 0.1 mM $CaCl_2$, and 0.1 M NaCl (*9*). The reaction mixture was incubated at 37 °C, and 9 μL of the reaction mixture was withdrawn at 0, 0.5, 1, 3, 6, and 24 h. The reaction was terminated by transferring each withdrawn fraction into a plastic tube containing 3 μL of 0.4% SDS, 100 mM Tris-HCl (pH 6.8), 800 mM glycine, and 5 mM PMSF on ice, followed by boiling for 3 min. The samples were then analyzed on 15% SDS−PAGE. For Edman degradation, proteins in the polyacrylamide gel were electrophoretically transferred to a PVDF membrane and stained with Coomassie Brilliant Blue R-250 (Wako). Pieces of the blotted membrane were directly analyzed with a protein sequencer (Applied Biosystems, Procise).

Thermal Unfolding Experiments. Intrinsic tryptophan fluorescence was evaluated to monitor the unfolding of the N-terminal domain of gpV, since gpV has tryptophan residues only in the N-terminal domain. Fluorescence was measured with a Hitachi F-4010 fluorescence spectrophotometer using an excitation wavelength of 290 nm and emission at 342 nm at a heating rate of 1 K/10 min. The protein concentrations used in the fluorescence measurements were 0.1 mg/mL for the wild type and Gly64Ala and 0.16 mg/mL for Gly64Leu in 2 mL of buffer containing 20 mM phosphate (pH 7.4) with 500 mM arginine to suppress aggregation.

Calorimetric measurements of gpV-C were performed to monitor the unfolding of the C-terminal domain of gpV and measured using a differential scanning calorimeter (VP Capillary-DSC, MicroCal), at a heating rate of 1 K/min (*10*). The protein concentration was adjusted to 2.0 mg/mL after dialysis against 20 mM phosphate (pH 7.4) and 500 mM arginine. The corresponding dialysis buffers were used as reference solutions for DSC measurements.

Analytical Ultracentrifugation. Analytical ultracentrifugation was performed in an Optima XL-I instrument (Beckman) with a four-hole An60Ti rotor at 20 °C with standard double-sector centerpieces and quartz windows. Sedimentation velocity experiments were conducted with 3.0 mg/mL gpV-C in 50 mM Tris-HCl (pH 7.4) and 500 mM arginine at a rotor speed of 40000 rpm. The acquired data were analyzed using SEDFIT (*11*) to determine the sedimentation coefficient and molecular mass. The partial specific volume, 0.7234 cm^3/g, was estimated from the amino acid composition of gpV-C using SEDNTERP (*12*). The solvent viscosity (1.31245 cP) and solvent density (1.0401 g/mL) at 20 °C were measured using an Ubbelohde capillary viscometer and a DMA-604 density meter (Anton-Paar), respectively.

Light Scattering Measurements. A vertically polarized argon ion laser operated at 488 nm was used as the incident beam for the light scattering measurements. The vertically polarized scattered light intensity was detected with a photomultiplier tube using the photon counting method. The size distribution of the dispersing particles was determined by means of correlation function measurements using an ALV-5000E correlator (*13*). A cylindrical cell with an outer diameter of 10 mm was placed in a thermostated silicon oil bath. The temperature was monitored using a calibrated platinum resistor. Optical purification of the sample solution was achieved by centrifugation (12000 rpm for 10 min) and filtration through nylon membrane filters with a pore size of 0.45 μm. The protein concentrations were 0.5, 1.0, and 2.0 mg/mL in a buffer of 20 mM phosphate (pH 7.4) containing 500 mM arginine to suppress aggregation. The scattered light intensity was analyzed by means of Zimm plots, and the molecular mass was evaluated (*14*).

Binding of gpV to E. coli Cell Membranes. The *E. coli* C strain (NBRC13891) was purchased from the National Institute of Technology. After cell harvest by centrifugation, the cells were resuspended in 50 mM Tris (pH 7.4) and sonicated. The cell membranes were recovered by centrifugation and resuspended in the same buffer. The binding reaction was performed by mixing gpV-C (20 μL of 0.19 mg/mL protein) and *E. coli* membranes (20 μL of 0.5 mg/mL protein) in 50 mM Tris (pH 7.4) and 1 mM $CaCl_2$ at 30 °C for 10 min. The concentration of *E. coli* membrane proteins was estimated using a protein assay kit (Bio-Rad). The cell membrane and bound proteins that had precipitated after

centrifugation at 12000 rpm for 10 min were separated from the supernatant. After the precipitant had been washed twice with 50 mM Tris (pH 7.4) and 1 mM $CaCl_2$, the amount of bound and unbound gpV on cell membranes was estimated using 15% SDS−PAGE.

A quartz crystal microbalance (QCM) was also used for the binding assay. This device measures mass change and molecular interactions on a crystal surface by measuring the change in frequency of a quartz crystal resonator. Resonance is disturbed by the addition of a small mass due to molecular interactions. Quartz crystals (9 MHz) with gold layer deposition areas of 1.96×10^{-1} cm^2 were used for the QCM measurements. The gold surfaces were cleaned with piranha solution [H_2SO_4/H_2O_2 (3:1, v/v)] for 15 min, rinsed with dioxane, and then immersed for 18 h at room temperature in a dioxane solution of 10 μM dithiobis-(succinimidyl hexanoate) (Dojin), to establish a self-assembling monolayer (SAM) containing active succinimidyl esters on the gold surface. The quartz crystal modified with the SAM layer was subsequently rinsed with dioxane, dried in air, and then placed in 200 μL cuvettes dipped in PBS. Prior to the binding measurements, *E. coli* membrane fractions (100 μL, 0.5 mg/mL protein) were injected into the system, immobilizing the membranes. Finally, after the crystal had been washed with PBS, concentrated gpV-C was placed in the cuvette to a concentration of 1 mg/mL and any changes in frequency were monitored. All of the QCM measurements were performed at 25 °C using a QCA922 device (Seiko EG&G), and the frequency of the quartz crystal oscillator was simultaneously recorded on a personal computer (*15*).

RESULTS

Expression and Purification of Full-Length gpV and Its Temperature-Sensitive Mutants. The pEE670 plasmid carrying the P2 gene V was constructed by E. Haggård-Ljungquist (*8*). Expression of gpV from pEE670 was observed in soluble fractions via SDS−PAGE and confirmed by N-terminal sequencing. It was reported that P2*ts*199 contains a mutation in gpV that changes Gly64 to Glu. Therefore, we attempted to express not only the wild type but also mutants Gly64Glu(*ts*), Gly64Lys, Gly64Ala, and Gly64Leu at 20, 30, and 37 °C for comparison. Wild-type, Gly64Ala, and Gly64Leu gpV were expressed very well at all temperatures. In contrast, Gly64Lys was expressed well at 20 °C but only slightly at 37 °C. Gly64Glu(*ts*) was expressed only at 20 °C and was observed less than the other gpVs on SDS−PAGE. N-Terminal sequencing demonstrated that Gly64Glu(*ts*) expressed at 20 °C had lost the N-terminal histidine tag (Figure 1). Wild-type, Gly64Lys, Gly64Ala, and Gly64Leu gpV were then expressed at appropriate temperatures and purified by anion-exchange, nickel-affinity, and gel-filtration chromatography. The purified fractions gave a single band on SDS−PAGE.

Limited Proteolysis of gpV. Limited proteolysis was conducted to probe the domain structure of gpV. Chymotrypsin cleavage of gpV gave rise to a stable intermediate fragment of 17 kDa and a 14 kDa protease-resistant fragment within 6 h (Figure 2). N-Terminal sequencing of these fragments showed that the N-termini of the 17 and 14 kDa products were Trp59 and Ser87, respectively. Thus, the N-terminal domain of gpV consisted of Met1−Tyr86 and was cleaved more rapidly than the C-terminal domain, indicating that the N-terminal region has a relatively flexible structure.

Thermostability Measurements of gpV and gpV-C. We attempted to compare the stability of the N-terminal and

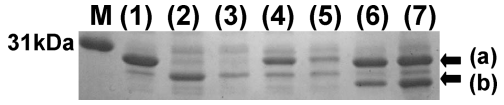

FIGURE 1: Expression of gpV and its mutants at 37 and 20 °C. Transformed BL21(DE3)pLysS cells were grown at appropriate temperatures in Luria broth containing 100 μg/mL ampicillin. Expression of gpV was induced with 1 mM IPTG when the turbidity at 600 nm reached 0.8. The cells were harvested by centrifugation after cultivation for a further 3 h, followed by sonication. Supernatants were recovered after centrifugation and subjected to 15% SDS−PAGE: lane M, molecular mass markers; lane 1, wild-type gpV at 37 °C; lane 2, Gly64Glu(*ts*) at 20 °C; lane 3, Gly64Glu(*ts*) at 37 °C; lane 4, Gly64Lys at 20 °C; lane 5, Gly64Lys at 37 °C; lane 6, Gly64Leu at 37 °C; lane 7, Gly64Ala at 37 °C; (a) gpV and mutants with a histidine tag; (b) mutants without a histidine tag.

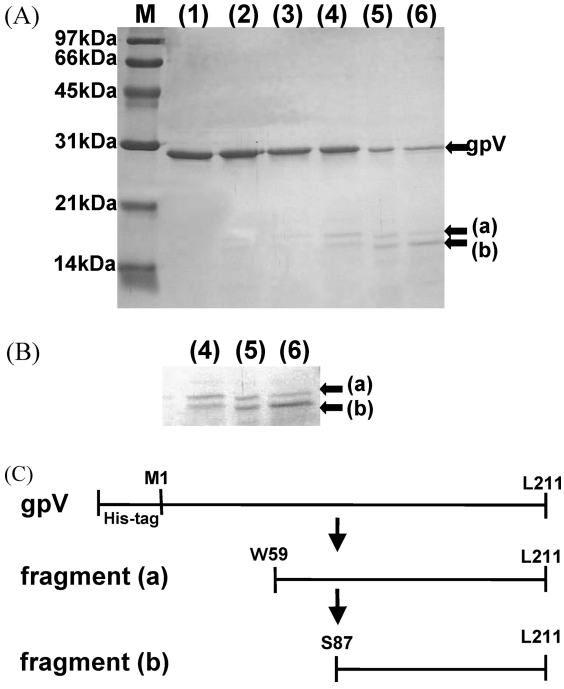

FIGURE 2: Limited proteolysis of gpV using chymotrypsin. (A) Chymotrypsin digestion was performed with a chymotrypsin:protein weight ratio of 1:50 at 37 °C. The samples were analyzed via 15% SDS−PAGE: lane M, molecular mass markers; digestion for 0 min (lane 1), 30 min (lane 2), 1 h (lane 3), 3 h (lane 4), 6 h (lane 5), or 24 h (lane 6); (a) fragment Trp59−Leu211; (b) fragment Ser87−Leu211. (B) Overexposed image at the region containing the protease-resistant fragments from panel A. (C) Schematic figure for the time course of limited proteolysis.

C-terminal domains of gpV. Since the recombinant N-terminal domain was insoluble, we did not purify and measure the thermostability of the N-terminal domain directly (Figure 3A). Four residues, Trp44, Trp47, Trp58, and Trp59, which comprise all of the tryptophan residues in gpV, form a cluster in the N-terminal domain. Thus, we considered that the intrinsic tryptophan fluorescence change of gpV corresponded to denaturation of the N-terminal domain. The fluorescence intensity gradually decreased at ~around 30−40 °C via a spontaneous temperature influence. In contrast, a significant and emergent decrease in fluorescence intensity was found in the region of 40−55 °C. Figure 4 indicates that the melting temperature (T_m) of wild-type gpV is ~50 °C. The *ts* site was mapped for Gly64Glu and was located close to the tryptophan cluster in the primary structure. Therefore, fluorescence observation was also useful for investigation of mutation effects at the *ts* site. The native *ts* mutant

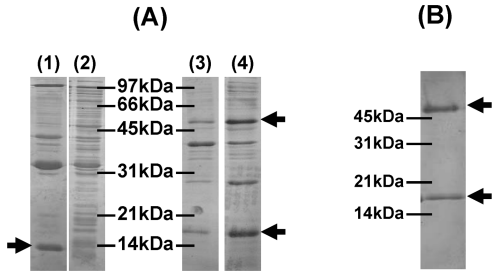

FIGURE 3: Expression of the gpV N-terminal fragment (Met1−Tyr86) and gpV-C (Ser87−Leu211). Samples were prepared and subjected to 15% SDS−PAGE as described in the legend of Figure 1. (A) Precipitant (1) and supernatant (2) fractions of an expression experiment for the N-terminal fragment (Met1−Tyr86) after sonication and centrifugation. The arrow corresponds to the N-terminal fragment (Met1−Tyr86). Precipitant (3) and supernatant (4) fractions of an expression experiment for gpV-C (Ser87−Leu211) after sonication and centrifugation. The arrows correspond to the monomer and trimer of gpV-C. (B) SDS−PAGE analysis of purified gpV-C (Ser87−Leu211). The arrows correspond to the monomer and trimer of gpV-C.

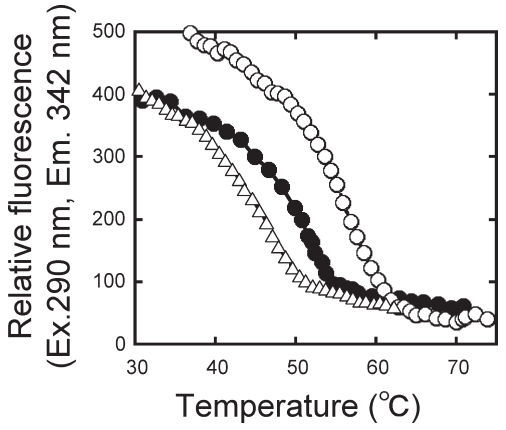

FIGURE 4: Fluorescence curves of gpV and its mutants. Fluorescence was measured with a Hitachi F-4010 fluorescence spectrophotometer using an excitation wavelength of 290 nm and emission at 342 nm, at a heating rate of 1 K per 10 min. The protein concentrations were 0.1 mg/mL for the wild type (●) and Gly64Ala (△) and 0.16 mg/mL for Gly64Leu (○) in 2 mL of 20 mM phosphate buffer (pH 7.4) containing 500 mM arginine to suppress aggregation.

Gly64Glu was expressed without the histidine tag (Figure 1) and was very unstable. In fact, spontaneous degradation of Gly64Glu occurred during purification, making it difficult to purify. The other mutants, Gly64Ala, Gly64Lys, and Gly64Leu, were purified using the same protocol as for the wild type, and their T_m values were measured by observation of florescence. The T_m for Gly64Ala was 46 °C, significantly lower than that of the wild type (Figure 4). Gly64Lys gave only a gradual decrease in fluorescence and showed no transition, indicating its denatured state (data not shown). Surprisingly, the T_m of Gly64Leu was approximately 56 °C, indicating that Gly64Leu is a more stable structure than the wild type (Figure 4). The gpV-C was purified (Figure 3B) and analyzed by DSC to determine the properties of the C-terminal domain. DSC measurements revealed a single peak, as shown in Figure 5. Rescanning DSC measurements did not give any peaks, indicating that the thermal denaturation process of gpV-C was irreversible. The irreversible DSC curve provides only the apparent T_m. The apparent T_m corresponding to the peak temperature was 72 °C, more than 20 °C higher than that of the N-terminal domain.

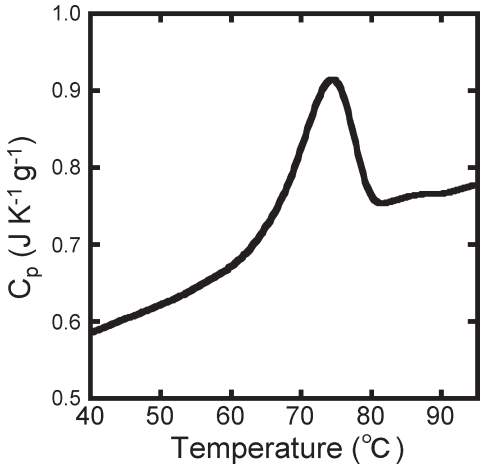

FIGURE 5: DSC curves for the thermal transition of gpV-C. Measurements were performed with a differential scanning calorimeter (VP Capillary-DSC, MicroCal) at a heating rate of 1 K/min. The protein concentration was 2.0 mg/mL in a buffer containing 20 mM phosphate (pH 7.4) with 500 mM arginine to suppress aggregation.

Determination of the Molecular Mass of gpV-C in Solution. Several preliminary experiments suggested that gpV had a very high molecular mass and formed aggregates very easily. However, these gpV aggregates often precipitated and could not be used for characterization. By contrast, although gpV-C showed a few peaks via gel-filtration chromatography, suggesting that it formed some aggregates, it did not form a precipitate and remained stable in solution. The material from the final peak was used for molecular mass determinations using two independent measurements. First, sedimentation velocity analysis was conducted (Figure 6A). The sedimentation coefficient of gpV was calculated to be 2.78 ± 0.096 S. The molecular mass was also estimated using SEDFIT and was observed to be 47.1 ± 2.3 kDa. This analysis also revealed aggregate species of gpV-C, but the aggregate population was less than 10% of the total. The molecular mass of gpV-C was also determined by static light scattering. Using a Zimm-Berry plot (*14*), the molecular mass was estimated to be 47.6 kDa. A positive slope corresponding to a positive second virial coefficient was found, suggesting significant intermolecular interactions (Figure 6B). The population of aggregate gpV-C species was estimated to be ~12% by dynamic light scattering measurements (data not shown). Both experiments revealed essentially the same results and are expected to be overestimates of the molecular mass, since gpV-C tends to self-associate. Judging from the calculated molecular mass of 14 kDa expected from the nucleotide sequence, we conclude that gpV-C forms a trimeric protomer in solution.

Membrane Binding Experiments. Initially, the binding of gpV-C to a crude *E. coli* membrane preparation was studied by coprecipitation experiments. In contrast to the fact that purified gpV-C is usually recovered in the supernatant after centrifugation, gpV-C was found in the precipitant with the membrane when purified gpV-C and *E. coli* membranes were mixed and then centrifuged (Figure 7). This result suggests that gpV-C bound to *E. coli* membranes and precipitated with them. In the same experiments, BSA did not bind to *E. coli* membranes but was found in the supernatant (data not shown). QCM measurements were performed to confirm binding of gpV-C to the crude *E. coli* membrane preparation (Figure 8). During immobilization of *E. coli* membranes on the SAM layer, an approximate 150 Hz decrease in the quartz crystal oscillator corresponded to the

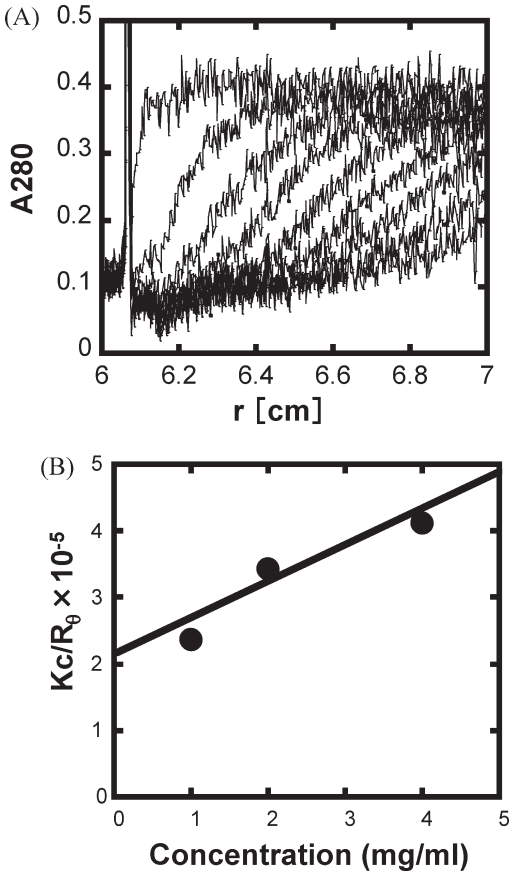

FIGURE 6: Measurements of the molecular mass of gpV-C. (A) Sedimentation velocity experiments for gpV-C. The moving boundaries were monitored by the absorbance at 280 nm at a rotor speed of 40000 rpm. Scans corresponded to a recording every 15 min. The molecular mass was estimated to be 47.1 kDa using SEDFIT (*11*). (B) Static light scattering at gpV-C concentrations of 1, 2, and 4 mg/mL was performed using a vertically polarized argon ion laser operated at 488 nm. Scattering light intensities were detected at a scattering angle of 30° with a photomultiplier tube using the photon counting method and analyzed by Zimm-Berry plots. From a reciprocal value of the *y*-axis intersection, the molecular mass was estimated to be 47.6 kDa.

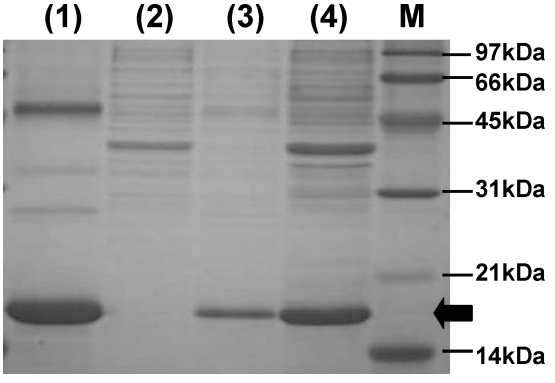

FIGURE 7: Observations of gpV-C binding to a crude *E. coli* membrane preparation by coprecipitation. An *E. coli* membrane fraction (20 μL of 0.5 mg/mL protein) and gpV-C (20 μL of 0.19 mg/mL protein) were incubated at 37 °C for 10 min and centrifuged. The supernatant and precipitant fractions were subjected to 15% SDS−PAGE: lane 1, gpV-C; lane 2, *E. coli* membranes; lanes 3 and 4, supernatant and precipitant of the coprecipitation experiment, respectively.

formation of covalent bonds between the SAM layer and approximately 150 ng of *E. coli* membranes (*15*). No frequency change occurred when another membrane fraction was injected. Thus, it appears that all of the reactive succinimidyl esters on the SAM layer were occupied by *E. coli* membranes. Finally, when gpV-C was injected into the cuvette, an additional decrease in frequency (approximately 80 Hz) and a significant increase in mass were observed. The fact that the mass did not decrease when the cuvette and quartz crystal were washed with PBS indicated that this reaction was irreversible. In contrast, injection of the same amount of bovine serum albumin did not cause an increase in mass. Although injection of cytochrome *c* caused a temporary increase in mass, the bound mass was removed when the cuvette and quartz crystal were washed with PBS. This suggests that an interaction between the positive charge on cytochrome *c* and the negatively charged *E. coli* membranes caused nonspecific binding. Membrane-bound gpV-C was also recovered in the precipitant in the expression experiments (Figure 3A, lane 3). We concluded that gpV-C was sufficient for binding of gpV to *E. coli* membranes.

DISCUSSION

The P2 phage consists of an isometric icosahedral head, a contractile tail, and tail fibers. The tail is composed of a sheath, tube, and baseplate containing tail spikes at the distal end of the head. Here, we analyzed the domain structure of the bacteriophage P2 gene V product, which was predicted to act as a tail spike in the baseplate. Limited protease digestion and N-terminal sequencing indicate that the N- and C-terminal domains consist of Met1−Tyr86 and Ser87−Leu211, respectively (Figure 2). One of the most interesting findings was that the N- and C-terminal domains exhibit very different stabilities. The N-terminal domain contains a *ts* site and a tryptophan cluster. Amino acid replacements at the *ts* site, Gly64, affected in vivo stability (Figure 1). Since the N-terminal domain was well expressed but recovered in the cell debris (Figure 3A), direct measurements of the T_m for the N-terminal domain were not feasible. As gpV contains a tryptophan cluster in the N-terminal domain and these tryptophan residues comprise all of the tryptophan in gpV, we employed tryptophan fluorescence measurements of full-length gpV to estimate the T_m of the N-terminal domain (Figure 4). These results indicated that the T_m of the N-terminal domain was approximately 50 °C and that additional electrostatic charges at the *ts* site caused by the Gly64Glu and Gly64Lys mutations were not conducive to its folding. In contrast to the N-terminal domain, the C-terminal domain purified easily and was stable, with an apparent T_m of 72 °C (Figure 5). It showed resistance to denaturation by sodium dodecyl sulfate (SDS) and remained a trimer in SDS−PAGE treatments (Figure 3B). Two other independent experiments also indicated that the C-terminal domain forms a trimer (Figure 6). This fact suggests that full-length gpV is a trimer, similar to other phage tail spikes, as described below. Our results also showed that the C-terminal domain binds to host cell membranes and that it functions in adsorption to the host (Figures 7 and 8).

Myoviridae are double-stranded DNA bacteriophages that have a long contractile tail with a baseplate. Tail spikes on the baseplate are also called short tail fibers. They are responsible for the attachment of the cell in the infection process and recognize the host bacterial cell surface. The best-studied short tail fiber is that of the bacteriophage T4, gp12. T4 gp12 forms a trimeric fiber and is attached to the baseplate by its protease-sensitive N-terminal domain, whereas a C-terminal domain binds to the cell (*16*). *Podoviridae*, the other family of DNA phages with very short noncontractile tails, also carry stubby tail spikes. Their tail

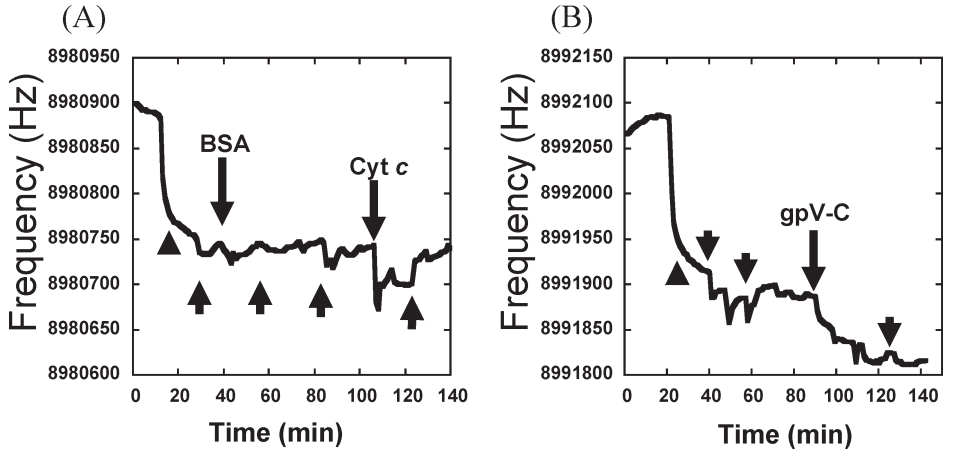

FIGURE 8: Observations of binding of gpV-C to a crude *E. coli* membrane preparation by QCM measurements. An *E. coli* membrane fraction (100 μL of 0.5 mg/mL protein) was injected into a 200 μL cuvette at the times denoted by the arrowheads. The cuvette was washed with 200 μL of PBS at the times denoted by the short arrows, and proteins (30 μL, 7.7 mg/mL) were injected at the times denoted by the long arrows (final protein concentration in the cuvette of 1 mg/mL). (A) Control experiments using bovine serum albumin (BSA) and cytochrome *c* (Cyt *c*). BSA exhibited no binding signal. Cytochrome *c* showed nonspecific binding and was dissociated by being washed with PBS. (B) Representative result of binding of gpV-C to *E. coli* membranes. We observed a decreasing frequency of approximately 150 Hz caused by immobilization of ~150 ng of *E. coli* membranes (arrowhead) and a change of 80 Hz corresponding to the specific binding of approximately 80 ng of gpV-C (long arrow) (*15*). The bound gpV-C did not dissociate with PBS washing (short arrow). All measurements were performed at 25 °C.

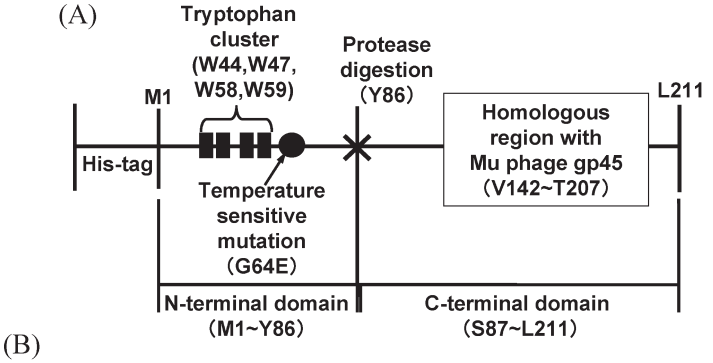

(B)

```
P2 gpV  142:VMVKASTRVTLDTPEVVCTNRLITGTLEVQKGG----TMRGNIEHTGGELSSNGKVLHTH: 197
Mu gp45 105:VTVKAAEKVTFDTPETEFTGNVTVQGDISGNGGMAVSARTGDSVTTGGDRVAGGISLRGH: 164

P2 gpV  198:KHPGDSGGTT: 207
Mu gp45 165:KHPGDSGGTT: 174
```

FIGURE 9: Summary of gpV domain structure. (A) Features of the primary structure domains. (B) Sequence homology in the C-terminal region of P2 phage gpV and Mu phage gp45. Homology matching performed using CLUSTAL W resulted in 45.5% similarity.

spikes not only are responsible for cell attachment but also hydrolytically cleave bacterial cell surface polysaccharides. This enzymatic activity is required for infection, but its function in the infection process is not well understood. Although the tail spike of bacteriophage P22, one of the best-studied podoviruses, is a very stable homotrimer, its N-terminal domain is thought to be flexible. Only the crystal structure of its protease-resistant C-terminal domain has been reported (*5*). The structures of the P22 tail spike and the trimeric receptor-binding domain for the tail spike proteins of the Det7 phage (*6*) and the short tail fibers of the T4 phage (*7*) have all been reported. The N-terminal domains of these tail spikes are thought to function in binding to their baseplates. Although P2 gpV has no significant homology to those structurally determined tail spikes, all of our results indicate that P2 gpV has typical features of phage tail spikes, such as a protease-sensitive N-terminal domain, a host-binding C-terminal domain, and a trimeric structure (Figure 9A). Thus, it is reasonable to surmise that the function of the N-terminal domain of P2 gpV contributes to baseplate assembly, similar to the other phage tail spikes. We also suggest that the N-terminal domain is flexible and less stable to allow induced fitting or a conformational change during baseplate assembly, since the Gly64Leu mutant, which has a T_m of ~56 °C, is much more thermostable than the wild type.

Furthermore, gpV may bind to lipopolysaccharide, similar to the tail spikes of P22, Det7, and T4. Conversely, membrane proteins such as OmpC and OmpF are also receptor proteins for many phages. In our preliminary experiments, we observed binding of gpV-C to crude *E. coli* membrane preparations from $OmpC^-$, $OmpF^-$, and $OmpC^-/OmpF^-$ *E. coli* strains using QCM measurements. Although we also detected the binding of gpV-C to lipopolysaccharide fractions that were treated with trichloroacetic acid, the details were not clear because of strong nonspecific signals in the QCM measurements (data not shown). Therefore, lipopolysaccharide is now the strongest candidate as the receptor molecule for gpV. Other methods in addition to QCM are necessary to confirm this, and we are in the process of developing these methods. The analysis of membranes prepared

from Mu phage-resistant strains is also a key in identifying gpV receptors. It is interesting that bacterial strains resistant to P2 are usually also resistant to Mu and P1, but not to most other phages (*17*). The Mu phage tail spike is annotated as the gene 45 product, gp45 (*18*). Although the overall level of identity between P2 gpV and Mu gp45 is not significant, their C-terminal regions are 45.5% identical (Figure 9B). We can reasonably speculate that the differences in sequence homology between the N-terminal and C-terminal domains reflect their different functions, contributing to baseplate assembly and host cell binding, respectively. Therefore, homologous regions of P2 gpV and Mu gp45 would bind to similar host receptors and contribute to cross-host binding activity. Identification of the host receptors and comparison of their three-dimensional structures will be important for understanding the infection process, our next goal. We have purified Mu gp45 and are ready to study it as well as P2 gpV. These results will be published in the very near future.

ACKNOWLEDGMENT

We thank Professor E. Haggård-Ljungquist (University of Stockholm) for the kind gift of plasmid pEE670. We also thank Professor Fumio Arisaka (Tokyo Institute of Technology, Tokyo, Japan) for his great help in the analytical ultracentrifugation experiments.

REFERENCES

1. Nilsson, A. S., and Haggard-Ljungquist, E. (2007) Evolution of P2-like phages and their impact on bacterial evolution. *Res. Microbiol. 158*, 311–317.
2. Kita, K., Kawakami, H., and Tanaka, H. (2003) Evidence for horizontal transfer of the EcoT38I restriction-modification gene to chromosomal DNA by the P2 phage and diversity of defective P2 prophages in *Escherichia coli* TH38 strains. *J. Bacteriol. 185*, 2296–2305.
3. Goldberg, E., Grinius, L., and Letellier, L. (1994) Recognition, attachment, and injection. In Bacteriophage T4 (Karam, J. D., Ed.) pp 347−356, American Society for Microbiology, Washington, DC.
4. Riede, I., Drexler, K., Schwarz, H., and Henning, U. (1987) T-even-type bacteriophages use an adhesin for recognition of cellular receptors. *J. Mol. Biol. 194*, 23–30.
5. Steinbacher, S., Seckler, R., Miller, S., Steipe, B., Huber, R., and Reinemer, P. (1994) Crystal structure of P22 tailspike protein: Interdigitated subunits in a thermostable trimer. *Science 265*, 383–386.
6. Walter, M., Fiedler, C., Grassl, R., Biebl, M., Rachel, R., Hermo-Parrado, X. L., Llamas-Saiz, A. L., Seckler, R., Miller, S., and van Raaij, M. J. (2008) Structure of the receptor-binding protein of bacteriophage det7: A podoviral tail spike in a myovirus. *J. Virol. 82*, 2265–2273.
7. Thomassen, E., Gielen, G., Schutz, M., Schoehn, G., Abrahams, J. P., Miller, S., and van Raaij, M. J. (2003) The structure of the receptor-binding domain of the bacteriophage T4 short tail fibre reveals a knitted trimeric metal-binding fold. *J. Mol. Biol. 331*, 361–373.
8. Haggard-Ljungquist, E., Jacobsen, E., Rishovd, S., Six, E. W., Nilssen, O., Sunshine, M. G., Lindqvist, B. H., Kim, K. J., Barreiro, V., and Koonin, E. V.; et al. (1995) Bacteriophage P2: Genes involved in baseplate assembly. *Virology 213*, 109–121.
9. Arisaka, F., Takeda, S., Funane, K., Nishijima, N., and Ishii, S. (1990) Structural studies of the contractile tail sheath protein of bacteriophage T4. 2. Structural analyses of the tail sheath protein, Gp18, by limited proteolysis, immunoblotting, and immunoelectron microscopy. *Biochemistry 29*, 5057–5062.
10. Kitazawa, D., Takeda, S., Kageyama, Y., Tomihara, M., and Fukada, H. (2005) Expression and characterization of a baseplate protein for bacteriophage Mu, gp44. *J. Biochem. 137*, 601–606.
11. Laue, T. (2001) Biophysical studies by ultracentrifugation. *Curr. Opin. Struct. Biol. 11*, 579–583.
12. Lebowitz, J., Lewis, M. S., and Schuck, P. (2002) Modern analytical ultracentrifugation in protein science: A tutorial review. *Protein Sci. 11*, 2067–2079.
13. Kita, R., Takahashi, A., Kaibara, M., and Kubota, K. (2002) Formation of fibrin gel in fibrinogen-thrombin system: Static and dynamic light scattering study. *Biomacromolecules 3*, 1013–1020.
14. Sedlak, M. (1996) in Light Scattering (Brown, W., Ed.) pp 120−165, Clarendon Press, Oxford, U.K.
15. Toyama, Y., Sakurai, M., Mochizuki, M., Masuda, Y., Kogure, H., and Kubota, K. (2006) Measurement of additive effects of cyclodextrins on fibrin gelation by using quartz-crystal microbalance. *Trans. Mater. Res. Soc. Jpn. 31*, 743–746.
16. Makhov, A. M., Trus, B. L., Conway, J. F., Simon, M. N., Zurabishvili, T. G., Mesyanzhinov, V. V., and Steven, A. C. (1993) The short tail-fiber of bacteriophage T4: Molecular structure and a mechanism for its conformational transition. *Virology 194*, 117–127.
17. Kutter, E. (2005) Molecular mechanisms of phage infection. In Bacteriophages: Biology and Application (Kutter, E., and Sulakvelidze, A., Eds.) pp 165−222, CRC Press, Boca Raton, FL.
18. Morgan, G. J., Hatfull, G. F., Casjens, S., and Hendrix, R. W. (2002) Bacteriophage Mu genome sequence: Analysis and comparison with Mu-like prophages in *Haemophilus*, *Neisseria* and *Deinococcus*. *J. Mol. Biol. 317*, 337–359.